2016

A pulsation analysis of K2 observations of the subdwarf B star PG 1142-037 during Campaign 1: A subsynchronously rotating ellipsoidal variable

Michael D. Reed
Missouri State University

A. S. Baran

R. H. Østensen

J. H. Telting

J. W. Kern
MSU Undergraduate

See next page for additional authors

Recommended Citation

Reed, M. D., A. S. Baran, R. H. Østensen, J. H. Telting, J. W. Kern, S. Bloemen, P. Blay et al. "A pulsation analysis of K2 observations of the subdwarf B star PG 1142-037 during Campaign 1: A subsynchronously rotating ellipsoidal variable." Monthly Notices of the Royal Astronomical Society 458, no. 2 (2016): 1417-1426.

Monthly Notices
of the
ROYAL ASTRONOMICAL SOCIETY
MNRAS **458,** 1417–1426 (2016) doi:10.1093/mnras/stw348

A pulsation analysis of *K2* observations of the subdwarf B star PG 1142-037 during Campaign 1: A subsynchronously rotating ellipsoidal variable

M. D. Reed,[1⋆] A. S. Baran,[2] R. H. Østensen,[3] J. H. Telting,[4] J. W. Kern,[1] S. Bloemen,[5] P. Blay,[6,4] T. Pursimo,[4] T. Kuutma,[4,7] D. Slumstrup,[4,8] M. Saajasto,[4,9] L. D. Nielsen,[4] J. Harmanen,[4,10] A. J. Winans,[1] H. M. Foster[1] and L. Rowe[1]

[1]*Department of Physics, Astronomy and Materials Science, Missouri State University, 901 S. National, Springfield, MO 65897, USA*
[2]*Suhora Observatory and Krakow Pedagogical University, ul. Podchorąży ch 2, PL-30-084 Kraków, Poland*
[3]*Instituut voor Sterrenkunde, KU Leuven, Celestijnenlaan 200 D, B-3001 Leuven, Belgium*
[4]*Nordic Optical Telescope, Rambla José Ana Fernández Pérez 7, E-38711 Breña Baja, Spain*
[5]*Department of Astrophysics/IMAPP, Radboud University Nijmegen, PO Box 9010, NL-6500 GL Nijmegen, the Netherlands*
[6]*Instituto Astrofisico de Canarias, C/Via Lactea, s/n, 38205 San Cristobal de La Laguna, Santa Cruz de Tenerife, Spain*
[7]*Tartu Observatory, Observatooriumi 1, 61602 Tõravere, Estonia*
[8]*Department of Physics and Astronomy, Stellar Astrophysics Centre, Aarhus University, Ny Munkegade 120, DK-8000 Aarhus C, Denmark*
[9]*Department of Physics, PO Box 64, FI-00014 University of Helsinki, Finland*
[10]*Department of Physics and Astronomy, Tuorla Observatory, University of Turku, Väisäläntie 20, FI-21500 Piikkiö, Finland*

Accepted 2016 February 10. Received 2016 January 27; in original form 2015 December 18

ABSTRACT

We report a new subdwarf B pulsator, PG 1142-037, discovered during the first full-length campaign of *K2*, the two-gyro mission of the *Kepler* space telescope. 14 periodicities have been detected between 0.9 and 2.5 hr with amplitudes below 0.35 parts-per-thousand. We have been able to associate all of the pulsations with low-degree, $\ell \leq 2$ modes. Follow-up spectroscopy of PG 1142 has revealed it to be in a binary with a period of 0.54 d. Phase-folding the *K2* photometry reveals a two-component variation including both Doppler boosting and ellipsoidal deformation. Perhaps the most surprising and interesting result is the detection of an ellipsoidal, tidally distorted variable with no indication of rotationally induced pulsation multiplets. This indicates that the rotation period is longer than 45 d, even though the binary period is near 13 h.

Key words: stars: oscillations – subdwarfs.

1 INTRODUCTION

K2 is the follow-up to the very successful *Kepler* space telescope mission, using the two surviving reaction wheels to stabilize the pointing (Howell et al. 2014). In this configuration, the spacecraft can reliably track targets at coordinates falling close to the ecliptic plane, where solar radiation pressure and regular thruster firings help keep the pointing to within a few pixels. Fields are mostly determined by pointing stability demands, in coordination with observer-proposed programmes. An observing *campaign* on any given field can last up to around 90 d. As with the original *Kepler* mission, observers must propose individual targets within the selected fields for long cadence (30 min) or short cadence (SC, 1 min) observations.

Our interest is asteroseismology of pulsating subdwarf B stars (sdB; also known as extreme horizontal branch stars), for which *Kepler* data have proven to be extremely useful. The near-continuous monitoring afforded by *Kepler* has revolutionized our ability to associate pulsation modes with pulsations. sdB stars pulsate in both gravity (V1093 Hya) and pressure (V361 Her) modes with periods near an hour or a few minutes, respectively. Most of the *Kepler*-observed sdB pulsators (sdBV) were g-mode pulsators (Østensen et al. 2010, 2011), some also with p-mode periodicities. The detection of evenly spaced g-mode periods (Reed et al. 2011) and rotationally induced frequency multiplets (Baran et al. 2012) has allowed most periodicities to be associated with modes, predominantly of low-degree $\ell \leq 2$. Discoveries from these data include slow rotation periods (see table 2 of Reed et al. 2014) even in <1 d binaries (Pablo, Kawaler & Green 2011; Baran & Winans 2012; Pablo et al. 2012), including one with differential rotation (Foster et al. 2015); some high-degree ($\ell \geq 3$) modes, including $\ell \geq 8$ (See fig. 9 of Telting et al. 2014b); some oscillations with stochastic

⋆ E-mail: mikereed@missouristate.edu

properties (Østensen et al. 2014a); and while evenly spaced periods indicate smoother core-envelope transitions than anticipated (see discussion in Reed et al. 2014), at least two sdB stars have trapped modes (Østensen et al. 2014b; Foster et al. 2015).

In preparation for the K2 mission, we made a selection of UV-bright targets falling near the ecliptic plane based on photometry from the *GALEX* satellite (Martin et al. 2005). The brighter of these targets were observed spectroscopically from the INT, Kitt Peak National Observatory (KPNO), Nordic Optical Telescope (NOT), and New Technology Telescope starting in 2014 January. The list contains 715 targets, and observations are ongoing, focusing on proposed K2 campaign fields.

Here, we report the discovery of a variable star from our analysis of K2's first campaign (C1) photometry, which spanned 93 d during 2014 May–August. The star, EPIC 201206621, is identified with PG 1142-037 (hereafter PG 1142) from the Palomar–Green survey which classified it as sdB-O with B = 15.67 (Green, Schmidt & Liebert 1986). It was observed using RC-Spec at the KPNO 4 m telescope during 2014 February as part of our spectroscopic programme described above. Two 900 s spectra were obtained which were sufficient to determine $T_{\rm eff} \sim 27\,000\,K$ and $\log g \sim 5.30$ using the same local thermodynamic equilibrium (LTE) models as described in Section 2.1, which placed it within the g-mode instability region. During 2014, PG 1142 was observed for 2.3 h to search for photometric variability by MDR. No pulsations were detected to a noise level of 8.1 parts-per-thousand (ppt). PG 1142 was listed in Reed & Stiening (2004) as not having a main-sequence companion earlier than M2 using 2MASS data.

2 OBSERVATIONS AND DATA PROCESSING

PG 1142 was observed by *K2* in SC mode which summed nine images into 58.8 s integrations. We downloaded pixel array files (15 × 14) from the Mikulski Archive for Space Telescopes. Unlike the main *Kepler* mission, K2 does not yet supply processed light curves, so investigators must extract fluxes from pixel data.

We used a set of custom scripts for extracting the light curve from the pixel files. First, we employed the PyFits library within PYTHON to read fits tables and pull out timestamps and fluxes. We limited data points to those having quality flag values of zero, therefore we avoided points affected by the onboard systematics. Secondly, we extracted light curves and stellar profile positions using the standard IRAF aperture photometry package PHOT after converting the pixel files into individual images using the KEPIMAGE program. This had the advantage that we could choose a small aperture which would follow the image centre using the IMCENTROID task. Since no flat fielding is applied to the data, we de-correlated the fluxes with stellar profile positions to remove the most disturbing feature present in K2 data, the roughly six hour periodicity caused by thruster firings to keep the spacecraft accurately pointed. This de-correlation was done on 10 d chunks of data. Finally, we removed long-term (>6 d) trends with Akima splines, normalized using the original median flux in each 10 d chunk, subtracted 1, and multiplied by 1000 to have differential fluxes in ppt.

We also processed the data using the PYKE (Still & Barclay 2012) software packages KEPMASK, KEPEXTRACT, KEPFLATTEN, and KEPCONVERT as well as the *K2*-developed KEPSFF. While these routines work well, we found that our techniques described above provide lower noise and so we did not use PYKE-processed data.

2.1 Spectroscopic parameters

Once pulsations were detected, we started observing PG 1142 spectroscopically as part of our campaign dedicated to investigating the binary status of pulsating hot subdwarfs observed by Kepler (e.g. Telting et al. 2014a). In 2015 February, March, and June, we obtained a total of 24 radial-velocity (RV) measurements of PG 1142, as listed in Table 1.

Table 1. Spectroscopic observations of PG 1142.

Date	BJD	S/N	RV	Error
2015-02-02T03:36:01.8	2457055.6539860	52.3	−20.037	5.674
2015-02-02T06:05:15.2	2457055.7576212	66.3	−92.296	7.049
2015-02-04T04:32:01.6	2457057.6930173	48.9	66.725	4.207
2015-02-04T06:23:54.7	2457057.7707205	55.7	21.640	7.752
2015-02-06T01:04:41.9	2457059.5491660	44.6	−97.101	6.922
2015-02-07T01:16:57.7	2457060.5577485	27.4	−66.534	10.827
2015-02-14T06:38:28.3	2457067.7814588	54.3	−47.224	5.931
2015-02-15T01:20:05.8	2457068.5604078	44.8	51.260	6.892
2015-02-15T05:12:26.7	2457068.7217691	27.1	−68.086	10.040
2015-03-01T23:31:21.3	2457083.4855331	46.9	−33.843	11.161
2015-03-02T02:33:37.4	2457083.6121128	50.0	74.737	7.231
2015-03-04T01:51:41.2	2457085.5830472	43.6	−91.444	5.336
2015-03-05T00:44:01.7	2457086.5360873	40.5	−64.897	6.872
2015-03-12T04:46:23.1	2457093.7045330	51.8	−82.345	5.677
2015-03-16T00:26:21.5	2457097.5239989	55.0	−59.301	4.197
2015-03-17T02:40:42.8	2457098.6173076	25.7	−49.665	7.195
2015-06-12T21:28:07.3	2457186.3951956	46.4	73.508	7.843
2015-06-12T22:46:09.4	2457186.4493808	55.7	80.049	6.347
2015-06-16T21:05:47.5	2457190.3793016	37.0	−29.492	6.194
2015-06-16T21:25:36.2	2457190.3930589	35.3	−25.492	8.038
2015-06-16T22:28:48.9	2457190.4369509	37.7	−55.445	6.903
2015-06-16T22:49:07.5	2457190.4510538	43.5	−62.600	6.493
2015-06-17T21:16:19.9	2457191.3865230	26.3	52.608	11.179
2015-06-17T23:14:12.0	2457191.4683685	56.4	−21.937	6.596

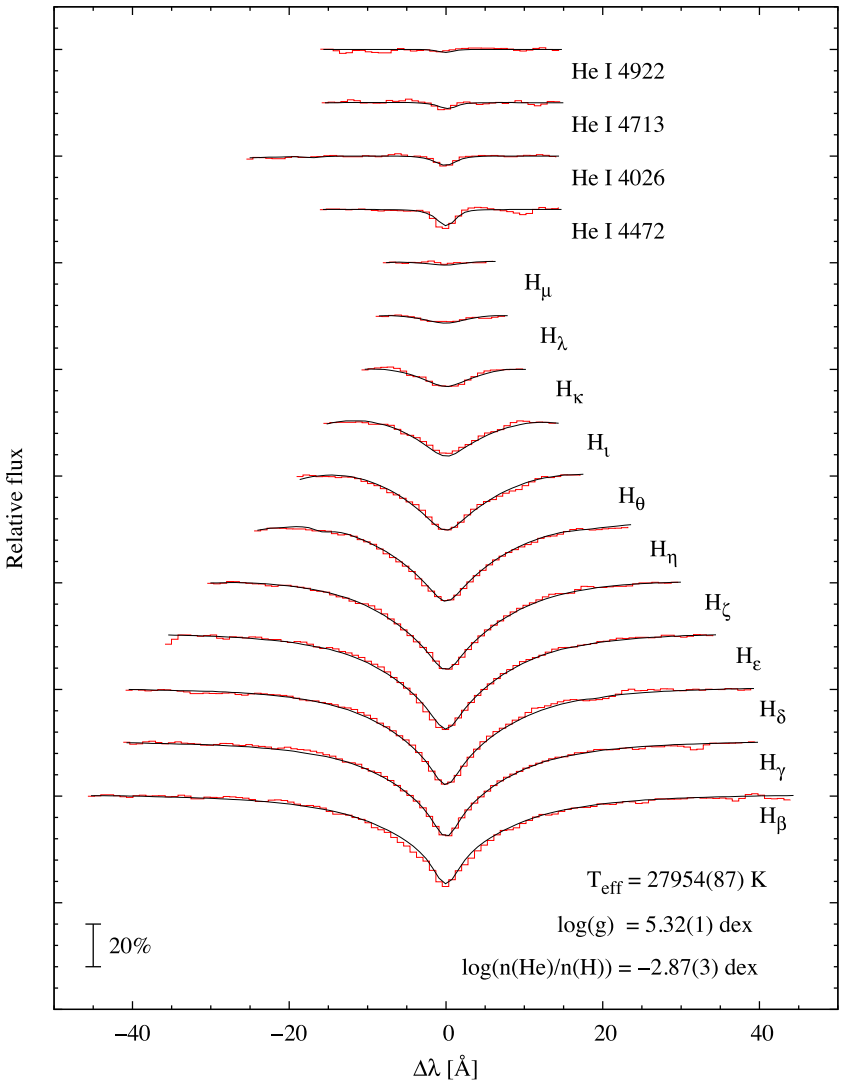

Figure 1. Fit to mean spectrum of PG 1142. Black lines show the fit while red ones the mean spectrum. Each line is labeled.

All low-resolution spectra were collected with the ALFOSC spectrograph at the NOT, using a 0.5 arcsec slit with the new high-efficiency volume-phased holographic grism #18, covering the approximate wavelength range of 3530–5200 Å, with resolution $R \sim 2000$ (or 2.2 Å) and dispersion of 0.82 Å pix^{-1}. The exposure time used was 900 s, except for one spectrum that was exposed 1500 s. The signal to noise (S/N) of the spectra ranges from 26 to 66, with a median value of 46, depending on observing conditions.

All spectra were processed and extracted using standard IRAF tasks. RVs were computed with FXCOR, by cross-correlating with a synthetic template derived from a fit to a mean spectrum of the target (see below), while using the H β, H γ, H δ, H 8, and H 9 lines from the observed spectra. After the first iteration, there was ∼4 per cent velocity residuals in phase with the signal and so we did an extra FXCOR iteration on spectra that were shifted to correct for the first RV results. This procedure led to a final RV amplitude about 4 per cent larger than obtained from the first try. The errors returned by the second FXCOR run are more consistent with the RMS from the orbit fit (see Section 3.2), so we used these errors for the analysis in this paper. The median RV error is 7 km s^{-1}.

The final RVs were adjusted for the position of the target on the slit, judged from slit images taken just before and after the spectra. Table 1 lists the observations with their mid-exposure dates, and RV measurements with the final FXCOR error.

We used the mean of the best 12 spectra (each with S/N>45), after shifting each to remove the orbit, and with final S/N∼180, to obtain the first high S/N determination of the atmospheric parameters of PG 1142. We determined $T_{\rm eff}$ and $\log g$ from the mean spectrum using the H/He LTE grid of Heber, Reid & Werner (1999) for consistency with Østensen et al. (2010). We used all the Balmer lines from H β to H 14 and the four strongest He I lines for the fit. We find $T_{\rm eff} = 27954 \pm 87$, K, $\log g = 5.32 \pm 0.01$, and $\log$ (N(He)/N(H)) $= -2.87 \pm 0.03$. The errors listed on the measurements are the formal errors of the fit, which reflect the S/N of the mean spectrum. These values and errors are relative to the LTE model grid and do not reflect any systematic effects caused by the assumptions underlying those models. The model fit is shown in Fig. 1.

3 DATA ANALYSIS

3.1 Pulsation analysis

93 d of near-continuous observations yields a $1/T$ resolution of 0.12 μHz, which is ∼71 000 independent frequencies up to the

Table 2. Periods detected for PG 1142. Column 1 provides an ID, columns 2 and 3 provide frequencies and periods with errors in parentheses. Column 4 lists the amplitude and Column 5 lists the corresponding S/N. Column 6 lists the mode degree with columns 7 and 8 listing a relative radial indices. Columns 9 and 10 list the deviation from the asymptotic sequence. No peaks attributed to spacecraft artefacts are listed in this table.

ID	Freq (μHz)	Period (s)	Amp (ppt)	S/N	ℓ	$n_{\ell=1}$	$n_{\ell=2}$	$\delta P/\Delta\Pi_1$	$\delta P/\Delta\Pi_2$
fA	21.37 (9)	46761 (188)	0.40						
fB	42.78 (7)	23377 (39)	0.26						
f1†	108.67 (9)	9199.6 (6.9)	0.12	3.5	2		57		−0.01
f2†	111.05 (9)	9004.7 (6.9)	0.13	3.8	1	31		−0.037	
f3	130.50 (7)	7663.1 (4.2)	0.21	6.2	1 or 2	26	47	−0.047	0.006
f4†	135.41 (9)	7396.4 (5.0)	0.13	3.8	1	25			−0.04
f5	157.38 (9)	6354.0 (3.7)	0.34	10.0	1	21		0.064	
f6	164.65 (8)	6073.6 (3.0)	0.26	7.6	1	20		0.017	
f7	223.82 (9)	4467.9 (1.8)	0.19	5.6	1	14		0.020	
f8	226.55 (8)	4414.0 (1.6)	0.19	5.6	2		26		−0.103
f9†	232.63 (12)	4298.7 (2.2)	0.13	3.8	2		25		0.148
f10	263.36 (8)	3797.1 (1.2)	0.19	5.6	2		22		−0.111
f11	273.25 (8)	3659.7 (1.0)	0.24	7.1	1 or 2	11	21	0.002	−0.003
f12†	296.12 (9)	3377.2 (1.0)	0.13	3.8	1	10		−0.050	
f13	296.50 (9)	3372.7 (1.0)	0.18	5.3	1	10		−0.070	
f14	297.44 (9)	3362.0 (1.0)	0.19	5.6	2		19		0.063

† these periodicities have low S/N in our final processing, but match asymptotic spacing and so were retained in our table.

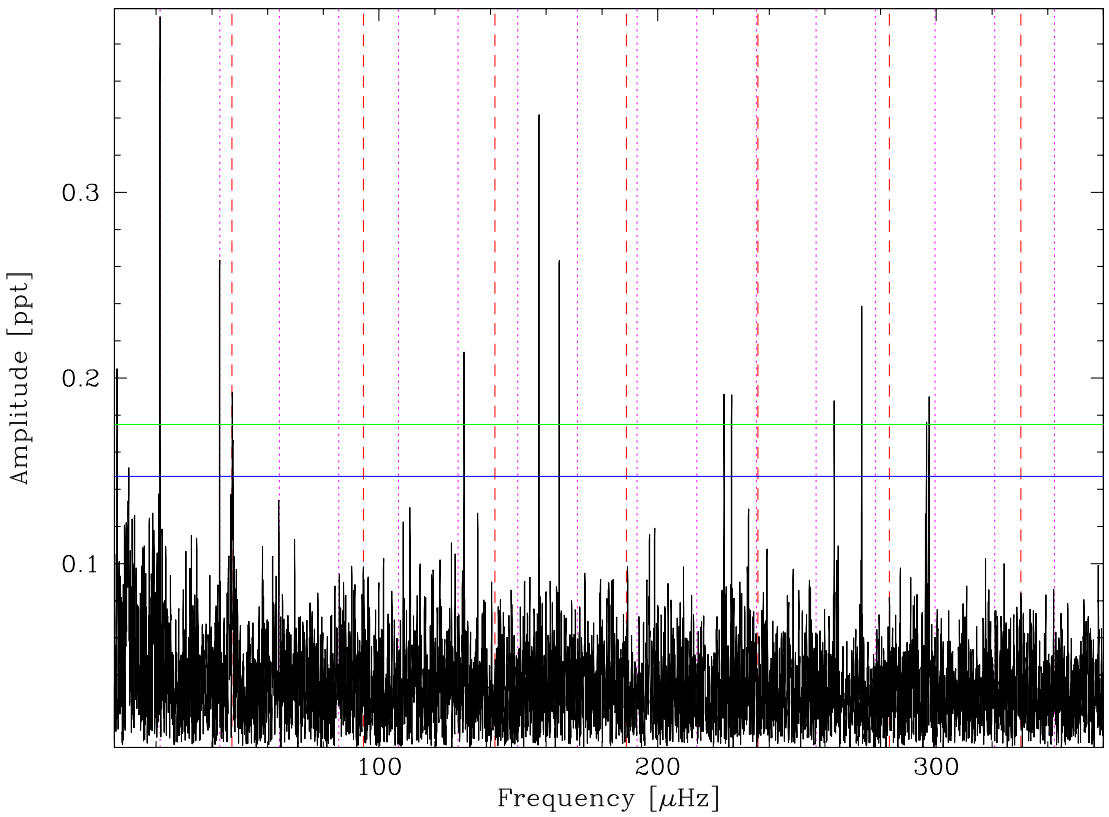

Figure 2. FT of PG 1142. Vertical dashed (red) lines indicate the 6 h thruster-firing periodicity and overtones and the dotted (magenta) lines indicate the binary period and its overtones. The horizontal lines indicate the 4.35σ and 5.2σ detection limits.

Nyquist. Initially, we used a detection threshold of 4.35σ (0.147 ppt) as indicated in Bevington & Robinson (2003) and then 5.2σ (0.175 ppt) as indicated in Baran, Koen & Pokrzywka (2015). However, having processed the data several times using multiple methods, we noted periodicities which were consistently distinguished from random noise. Using the higher detection limit to construct period sequences (described below), we noticed that the lower amplitude periodicities also fit into the sequences, and so retained them, even though they fall below a justifiable detection limit. We include the S/N values in Table 2 and note those frequencies with low values.

To determine the pulsation frequencies, amplitudes, and errors, we fitted Lorentzian profiles to the peaks of the FT (Fig. 2). This has become our standard procedure when pulsations have substantial

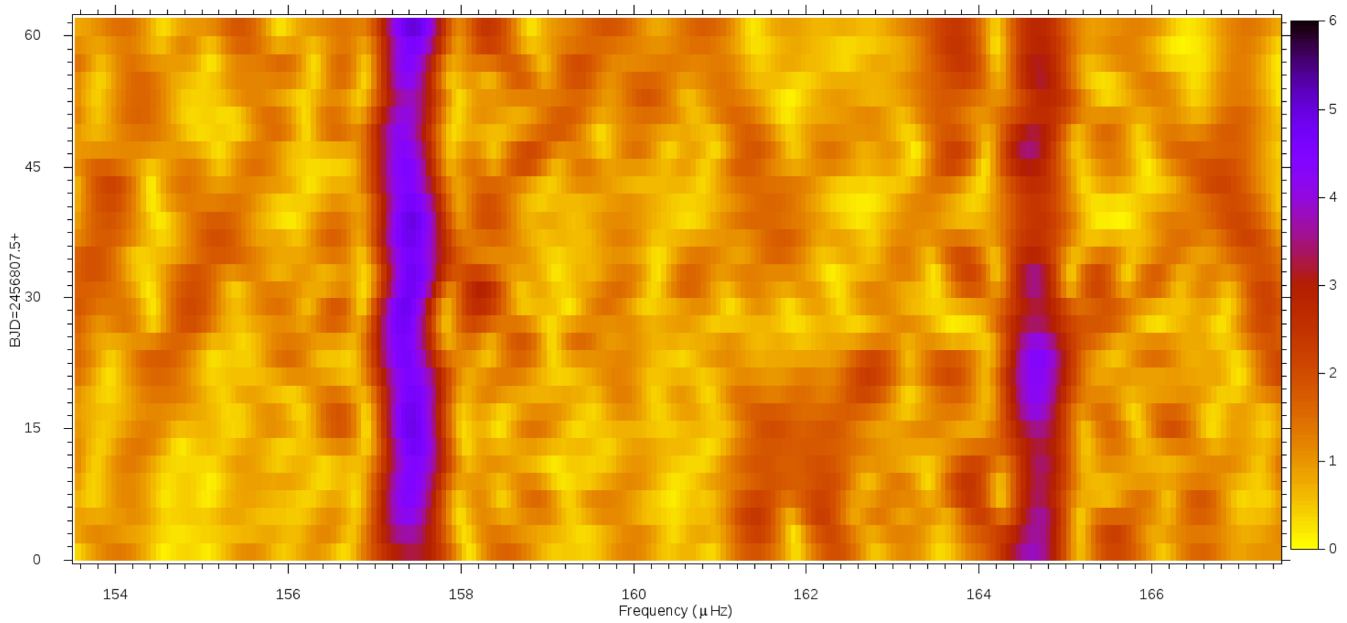

Figure 3. Sliding FT of the two highest amplitude periodicities showing amplitude variability. Frequency is on the abscissa and time on the ordinate with colour indicating the amplitude, in σ with a scale bar on the right. Each FT spans 20 d of data with each element sliding by 2 d.

amplitude and/or frequency variability. The previous method of non-linear least-squares fitting and pre-whitening is no longer effective as it assumes constant amplitudes, phases, and frequencies while the observations obviously do not possess these properties. Fig. 3 shows a sliding Fourier transform (FT) of the two highest amplitude periodicities, for reference. We do not wish to imply that the pulsations are stochastically excited (see Reed et al. 2007; Østensen et al. 2014a, for discussions), but use this tool as the most effective for determining frequency centres with the Lorentzian widths providing an indicator of line variability, regardless of its cause. The fitted periodicities are listed in Table 2 with other asteroseismically interesting quantities (described below).

The FT has 12 peaks above a $5.2\,\sigma$ detection limit. Three of these have long periods at 21.4 μHz (12.99 h), its overtone at 42.8 μHz and another at 47.8 μHz, which is the residuals of the thruster firings (not included in Table 2). Five other frequencies persistently appeared near 4σ through our various reductions. All of these occur near period spacing sequences (see discussion below) and so we include them in Table 2. Fig. 2 shows the FT with noise limits, artefacts, and binary signals and overtones indicated.

No consistent rotationally induced frequency multiplets appear in these data, so we can only use asymptotic period spacings for mode identifications. A Kolmogorov-Smirnov (KS) test statistic was calculated using the periods in Table 2 with the results shown in Fig. 4. From previous work with sdBV stars, we know that the $\ell = 1$ sequences should appear near 250 s and the $\ell = 2$ sequence should appear near 150 s (Reed et al. 2011), and indeed the strongest KS statistic appears near 265 s. Differencing the periods indicated that most of PG 1142's periods are separated nearly by this value or a multiple of it. The sequence was then determined by assigning a relative overtone, n, and calculating a linear regression of those periods and overtones. That fit was then used to find additional periods which fit the sequence. Nine of the 14 periods fit into this sequence with errors below 7 per cent. According to asymptotic theory (see Aerts, Christensen-Dalsgaard & Kurtz 2010), the $\ell = 2$ sequence is related to the $\ell = 1$ sequence as $\Delta\Pi_{\ell=2} = \Delta\Pi_{\ell=1}/\sqrt{3}$

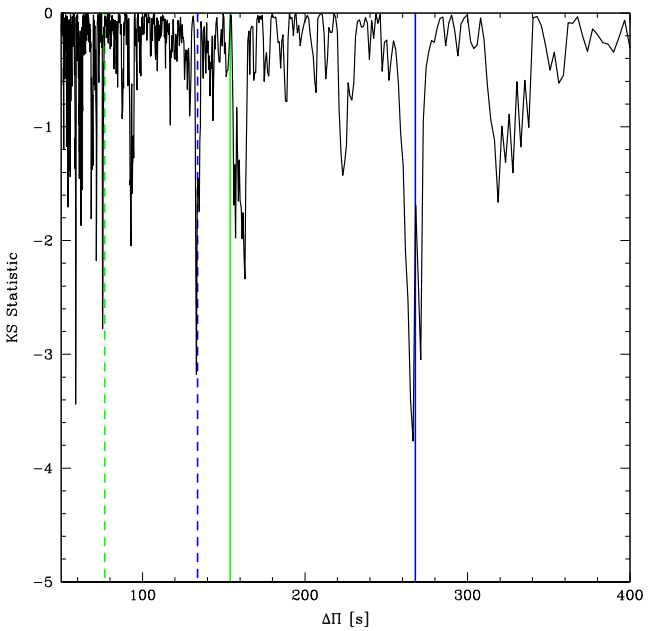

Figure 4. Period spacing sequences indicated by the KS test. The solid blue (green) line indicates the $\ell = 1$ (2) period spacing sequence with the dashed line the overtone alias.

and so we could determine which periods should be $\ell = 2$. Seven periods could be associated with the $\ell = 2$ sequence, including two peaks which also fit the $\ell = 1$ sequence. We cannot distinguish between $\ell = 1$ or 2 for these peaks (f3 and f11) and so Table 2 has listings for both. Fig. 5 shows a period transform with the resultant asymptotic period sequences indicated. The linear regression solutions find period spacing sequences of 267.9 ± 1.0 and 153.9 ± 0.7 s for the $\ell = 1$ and 2 sequences, respectively. This results in all periodicities being identified with spacings similar to other *Kepler*-observed g-mode pulsators (Reed et al. 2011).

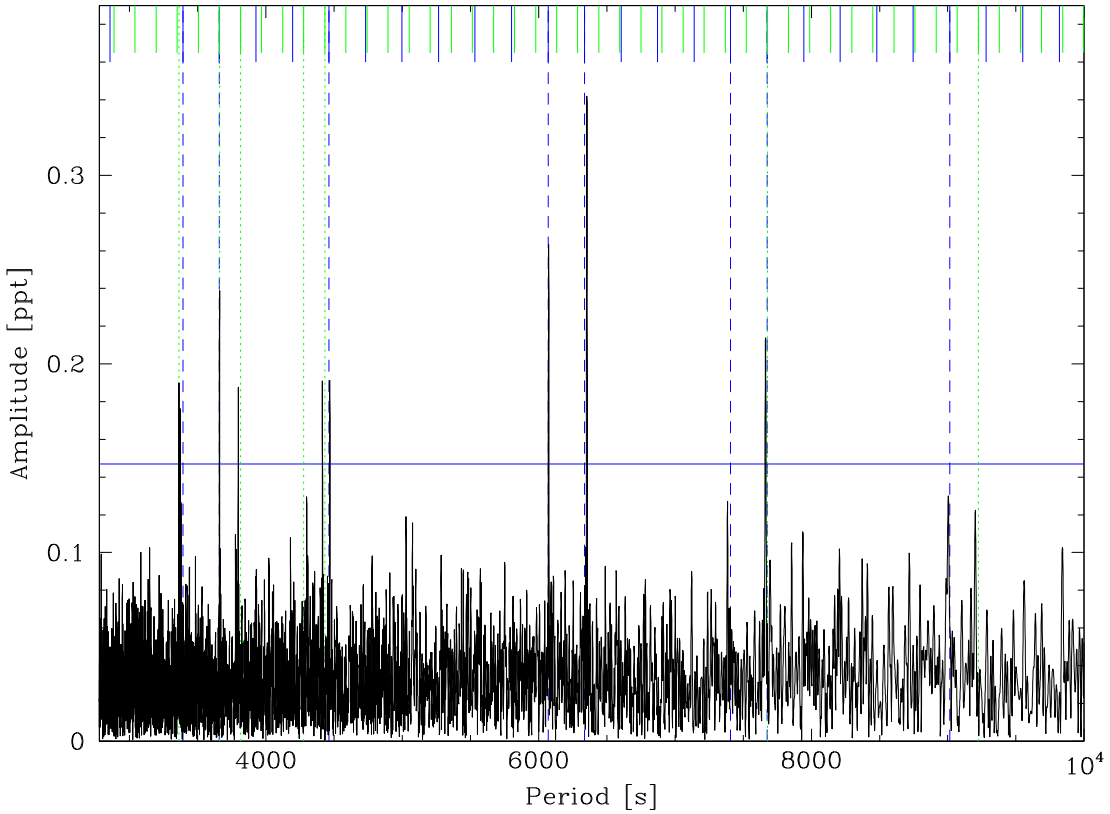

Figure 5. Period transform of PG 1142 showing evenly spaced periods. Short blue (green) lines indicate the asymptotic $\ell = 1$ (2) sequence with full-length lines indicating those which match detected periodicities. The horizontal line indicates 4.35σ for reference.

3.2 Binary analysis

PG 1142 has proven to be a very exciting target. The detection of fA and fB prompted follow-up spectroscopic observations (described in Section 2.1) to search for velocity variations, which were subsequently detected. Fitting the 24 RVs (in Table 1), and assuming a circular orbit, gives an orbital solution period of 0.541089 ± 0.000020 d (21.39 μHz), amplitude of 85 ± 2 km s^{-1}, and phase of BJD = $2457099.74105 \pm 0.00204$ (top panel of Fig. 6). The eccentricity was subsequently fitted at 0.079 ± 0.028, showing it is negligible for our calculations. Using the values of $K = 85 \pm 2$ km s^{-1} and P = 0.541 d from spectroscopy, the sdB canonical mass M1=0.47 and assuming $i = 90^o$, we get the minimum values for M_2 of 0.26 $M_\odot$ and for the orbital separation $a = a_1 + a_2 = 2.52\,R_\odot$. Of course we know this is not the inclination as no eclipses are evident in the light curve.

We attempted several phase-folding and binning combinations of the photometry to improve the period and phase, however the thruster firings, at roughly every six hours, and pulsations decrease the accuracy, and so the RV data are better for constraining the period. Still, the photometry show evidence of two-component variations, occurring at similar levels, in agreement with the FT. From the phasing of the variations, we can deduce the sources. A reflection-effect companion in the binary would produce a reflection-effect maximum, which would occur during a Doppler boosting zero-point (halfway between maximum and minimum) or an ellipsoidal-effect minimum. A Doppler boosting maximum would occur during an ellipsoidal-variable maximum. Figs 7 and 8 show the results of two-component fits to the folded light curve (described below). The phasing indicates that the components are Doppler boosting and ellipsoidal variations. These two components indicate that PG 1142 is most likely an sdB+WD binary.

We do not notice any eclipses in the folded light curve and the fitted Doppler and ellipsoidal amplitudes closely match the peaks in the FT, indicating that there is no additional contribution from eclipses. Using $R_{sdB} = 0.15\,R_\odot$ we calculate the inclination to be less than 87°. As PG 1142 is likely an sdB+WD binary, if we use the canonical WD mass of 0.6 $M_\odot$, we calculate an inclination of 35° and $a = a_1 + a_2 = 2.85\,R_\odot$. These properties are summarized in Table 3.

A simple two-component sine fit was done to the phase-folded and binned light curve as shown in Fig. 7. The resulting solution (included in Table 3) has a reduced $\chi^2 = 1.08$ and fitted the ellipsoidal amplitude at 0.25 ± 0.02 ppt and the Doppler boosting at 0.38 ± 0.02 ppt. From the RV amplitude of 85 km s^{-1} and following the procedure of Telting et al. (2012), the Doppler boosting can be calculated to be 0.39 ppt, which closely matches the photometric amplitude. The phasing of the Doppler and ellipsoidal signals appear exactly as expected in phase: maximum Doppler boosting coincides with an ellipsoidal maximum and the Doppler minimum with the other ellipsoidal maximum. This indicates that we are correctly interpreting the causes of variations.

We have also modelled the binary light curve using the LCURVE code (Copperwheat et al. 2010). We tested two scenarios with very different component masses, but both consistent with the measured orbital period and RV amplitude of the sdB. We assumed a white dwarf radius of $R_{WD} = 0.013\,R_\odot$ and an effective temperature of 27 000 K for the sdB and 20 000 K for the white dwarf. Limb darkening and gravity darkening coefficients do not have a large

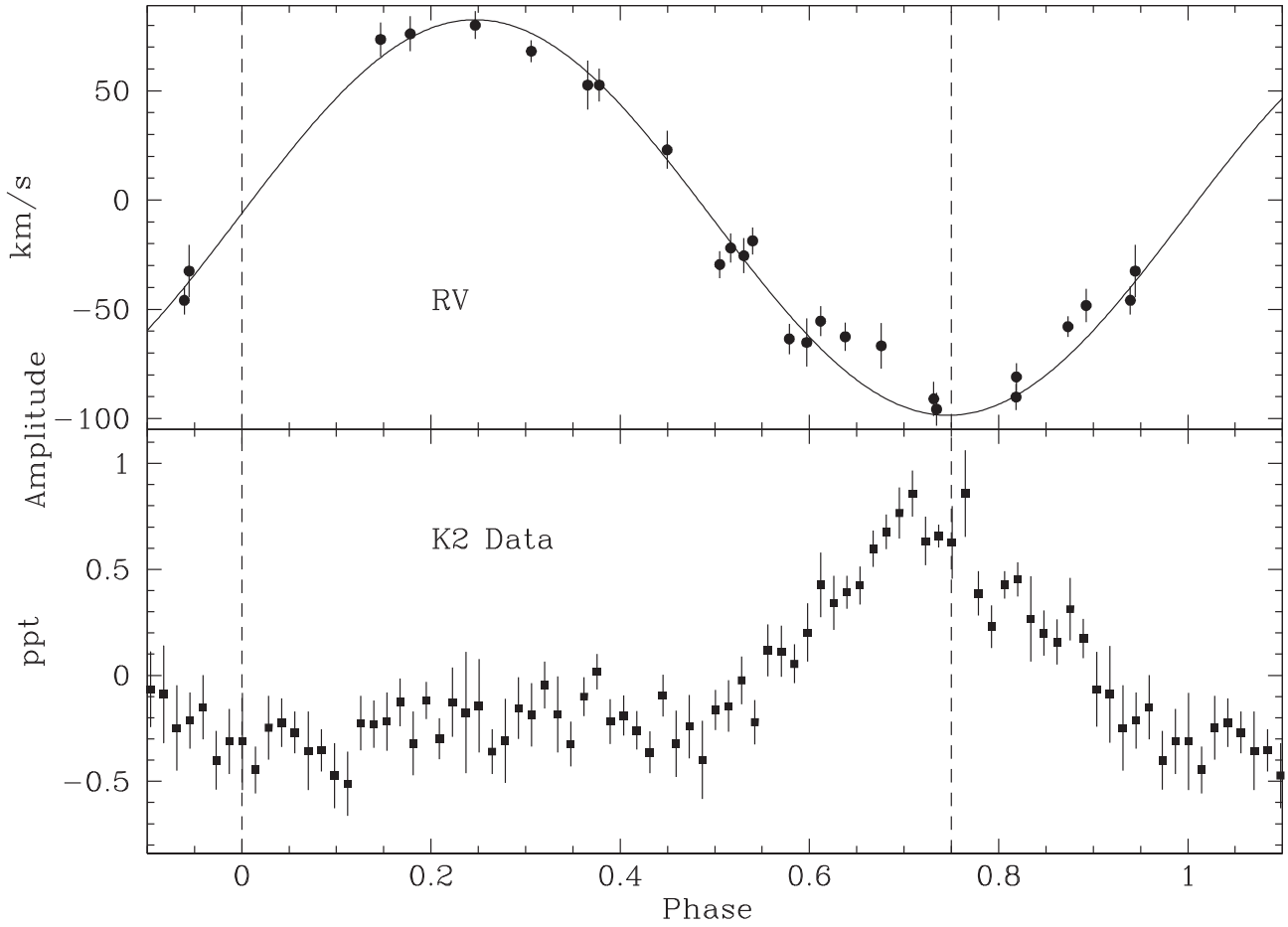

Figure 6. Velocity and photometric data folded over the orbital period. The K2 data have been phase-binned into 72 bins with 1σ error bars shown.

Table 3. Summary of spectroscopic and binary properties of PG 1142.

Property	Value	Comments
$T_{\rm eff}$	27954(54) K	Combined spectrum
log g	5.32(1) dex	Combined spectrum
log (n(He)/n(H))	−2.87(3) dex	Combined spectrum
Period	0.541089(20) d	RVs, circular orbits
K	85(2) km s^{-1}	RVs, circular orbits
Reduced χ^2 of the fit	1.4071	RVs, circular orbits
Fit RMS	7.8932	RVs, circular orbits
e	0.079(28)	RVs
$(a_1 + a_2)_{\rm min}$	2.52 R$_\odot$	$i = 90°$, $M_{\rm sdB} = 0.47$ M$_\odot$
$(M_2)_{\rm min}$	0.26 M$_\odot$	$i = 90°$, $M_{\rm sdB} = 0.47$ M$_\odot$
$i_{\rm max}$	87°	No observed eclipses.
$(a_1 + a_2)_{\rm canonical}$	2.85R$_\odot$	$M_{\rm sdB} = 0.47$ M$_\odot$, $M_{\rm WD} = 0.60$ M$_\odot$
$i_{\rm canonical}$	35°	$M_{\rm sdB} = 0.47$ M$_\odot$, $M_{\rm WD} = 0.60$ M$_\odot$
$A_{\rm ellipsoidal}$	0.25(2) ppt	Folded light-curve fit.
$A_{\rm Doppler}$	0.38(2) ppt	Folded light-curve fit.
Reduced χ^2 of the fit	1.08	Folded light-curve fit.

effect on the light curves and were fixed at the values used for KPD 1946+4340 in Bloemen et al. (2011). For Scenario 1, we used a white dwarf mass of 0.6 M$_\odot$ and an sdB mass of 0.47 M$_\odot$. These masses imply a mass ratio of $q = 0.78$, and an inclination of $i = 34.6$ deg. By fitting only the sdB radius, we found a best fit for $R_{\rm sdB} = 0.228$ R$_\odot$. The best model has a reduced $\chi^2 = 1.13$, which indicates that the model nearly perfectly explains the features in the observed light curve. For Scenario 2, we changed the white dwarf mass to 0.3 M$_\odot$ and kept the sdB mass at the canonical value of 0.47 M$_\odot$, which implies a mass ratio of $q = 1.57$ and a very different inclination of $i = 65.6$ deg. We found a best fit for $R_{\rm sdB} = 0.187$ R$_\odot$, resulting in a light curve with reduced $\chi^2 = 1.15$ which was nearly indistinguishable from the best fit in Scenario 1. Both fits are shown in Fig. 8. From this test, we conclude that sensible system parameters can explain the observed RV curve and K2 light curve, but in the absence of eclipses, model fitting the light curve does not provide useful constraints on crucial parameters such as the white dwarf mass and the inclination of the system.

4 RESULTS AND DISCUSSION

We discovered PG 1142 to be a new sdB pulsator from 93 d of K2 data obtained during C1. In the photometry we detect 14 periodicities associated with pulsations and two others related to binarity. Using asymptotic period spacing, we were able to identify all the pulsations as low-degree $\ell \leq 2$ modes.

One of our more surprising results is the *lack* of periodicities in the data, compared to other sdB pulsators. With 93 nearly continuous days of data, we were expecting to find more periodicities. Of the 13 g-mode sdBV stars discovered using 30 d of data during *Kepler's* survey phase (Østensen et al. 2010, 2011), only three, all fainter than PG 1142, had fewer periodicities and even EQ Psc,

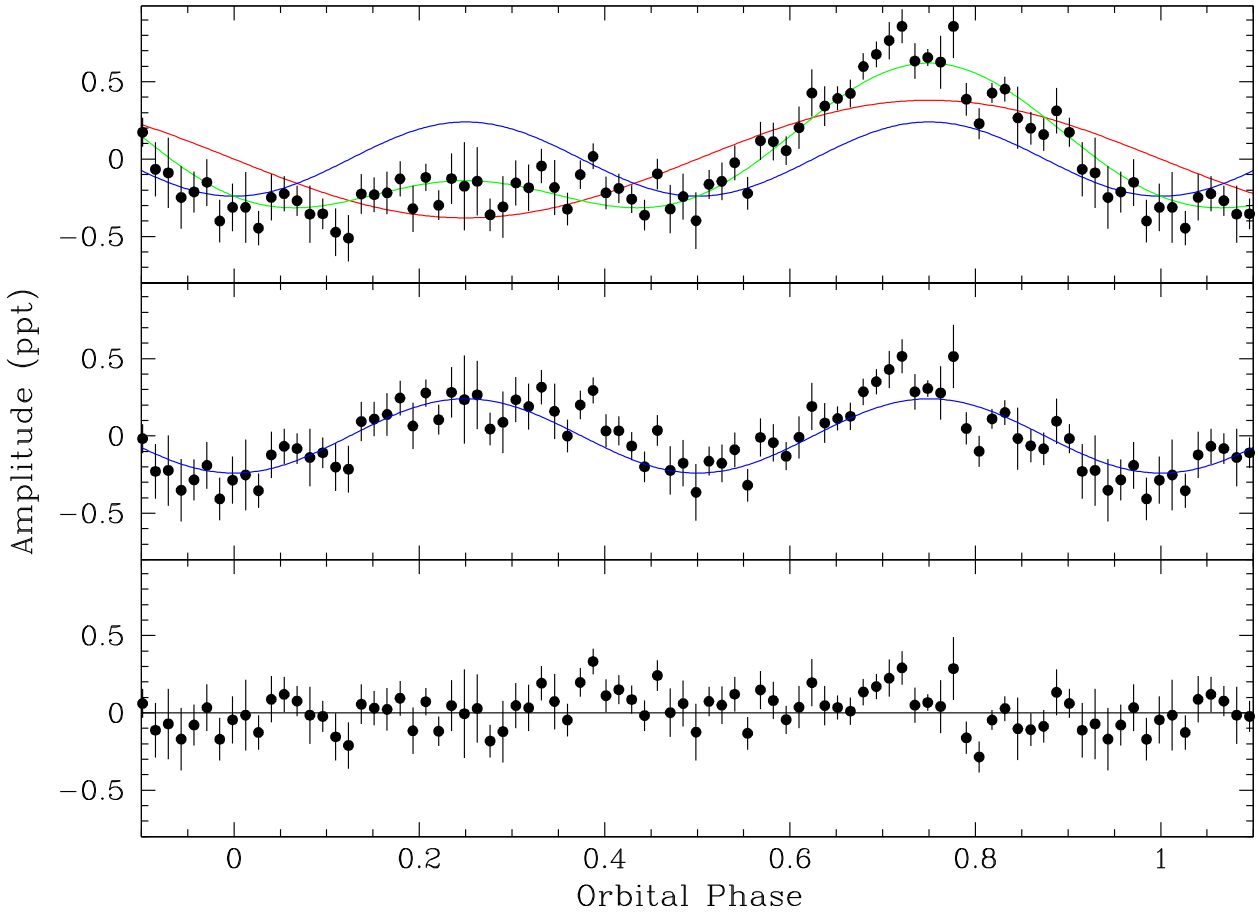

Figure 7. Orbital elements removed from the light curve. Top panel shows original folded and binned light curve. Orbital fits are indicated by lines with green being the combined fit, blue the ellipsoidal deformation, and red the Doppler boosting. Middle panel shows the Doppler-corrected light curve (with ellipsoidal deformation model) and the bottom panel shows the residuals after both elements have been removed.

using only nine days of K2 engineering data, shows more periodicities (Jeffery & Ramsay 2014). Fig. 9 shows the number of g-mode pulsations detected from *Kepler* survey-phase and K2 engineering observations. It would be expected that fainter stars would show fewer periods, having reduced S/N, and there is a very slight trend in that direction. Flux from (non-white dwarf) companions could also reduce the number of pulsations detected and the point types in the figure indicate those with companions. Again, it is mildly suggestive that companion flux impacts the results. Position within the instability strip could also affect the number of pulsations observed and so the right-hand panel indicates the number of pulsations observed against $T_{\rm eff}$. No obvious trend occurs. While it was expected that K2 data would have more noise than the main mission, these data contain three times as many points as survey-phase data, which should more than make up for the reduced S/N of individual measurements. As such, we are left to conclude that PG 1142 is one of the more sparse pulsators observed by the *Kepler* space telescope.

We also do not detect any obvious rotationally induced frequency multiplets. If PG 1142 were tidally locked, the 0.54 d orbit would produce $\ell = 1$ and 2 splittings in multiples of 10.7 and 17.8 μHz, respectively. The frequency differences appear roughly random and no frequency differences are within 1 μHz of the expected separations. Since all the frequencies (with the possible exception of f12) fit period sequences, the most likely explanation is that no frequency multiplets exist. This is suggestive that PG 1142 spins longer than ∼45 d. It is possible that f13 and the low-amplitude f12 form an $\ell = 1$ doublet. If this is the case, then the 0.40 μHz separation would indicate a spin period of 14.6 d. While we feel this is unlikely and f12 is most likely a spurious frequency, it would still be subsynchronous to the binary period. Of the nine known rotation periods of sdBV stars observed with *Kepler* and listed in table 1 of Reed & Foster (2014, and references therein), four would surely have been detectable from K2 data with three more having periods right around 45 d, which likely would have been detected. Only two have spin periods commensurate with the length of K2's C1, making it unlikely multiplets would have been detectable with these data. From our experience with *Kepler* and sdB variables, only extremely low-inclination angles suppress multiplets (see Reed et al. 2004, for example) and for any reasonable range of masses, the resultant orbital inclinations are well suited for detecting rotationally induced multiplets. As such, the lack of observed multiplets indicate that PG 1142 has a long rotation period of at least 45 d.

From spectroscopy and the folded light curve, we determined that PG 1142 is in a close binary with a period of 0.54 d. We measured a Doppler boosting amplitude of 0.38 ppt which matches the orbital velocity of 85 km s^{-1}. We also measured an ellipsoidal variable amplitude of 0.25 ppt. As we do not see eclipses, the inclination must be $< 87^\circ$ and, assuming canonical sdB and WD masses, we calculated an inclination of $i = 35^\circ$. At this inclination, multiplets should be easily observed if the rotation were commensurate with the orbital period. With the complete lack of observed multiplets implying a long rotation, this system is an excellent test for various

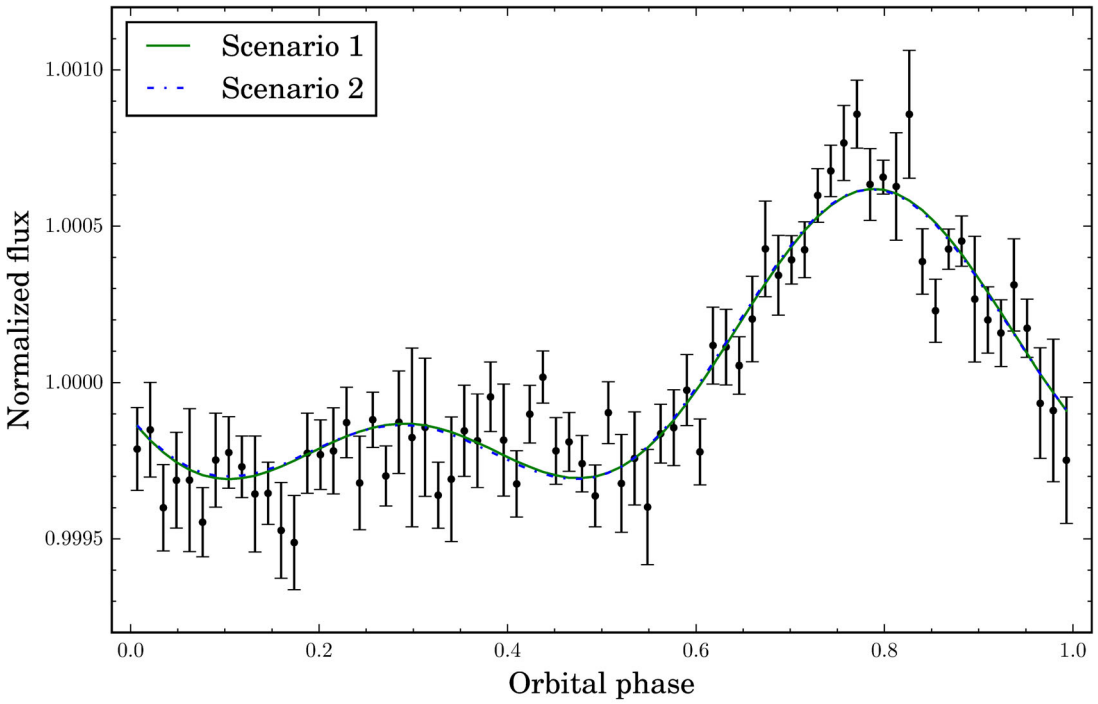

Figure 8. Model fits to the K2 light curve using the RV amplitude as a constraint. As discussed in Section 4, both fits use the canonical sdB mass of 0.47 $M_{\odot}$, Scenario 1 has a white dwarf mass of 0.3 $M_{\odot}$ and Scenario 2 has a white dwarf mass of 0.6 $M_{\odot}$. Both sets fit equally well.

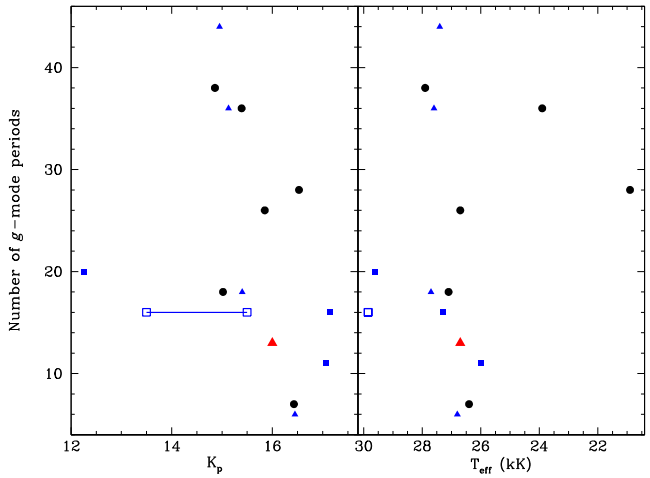

Figure 9. Number of g-mode pulsations detected with brightness and $T_{\rm eff}$ during *Kepler's* survey phase (summarized in Reed et al. 2011), or K2's engineering campaign for EQ Psc (open square; Jeffery & Ramsay 2014). Squares indicate sdB+dM binaries, triangles sdB+WD binaries, and circles single stars. PG 1142 is the red triangle. Note that the K_p magnitude for EQ Psc is listed as 15.5 while it is known to be about 2 mag brighter. Both values are indicated, connected by a line.

tidal locking mechanisms (e.g. Pablo et al. 2012) and, so far as we know, it is the first ellipsoidal variable which is likely rotating subsynchronously. With a rotation period >45 d, PG 1142 has the longest period of our known subsynchronously rotating binaries; a particularly surprising result as it is the only one with tidal deformation indicative of a stronger gravitational field from the companion.

Our results for PG 1142 represent very useful data points to complete our understanding of sdB stars, and by extension, the cores of red clump and other horizontal branch stars. The 14 observationally identified modes will present challenges for model fitting. Even four years after our first examination of *Kepler* data, there are *no* model fits using observationally constrained mode identifications. Once structural models accurately indicate the internal structure (via asteroseismology matching), PG 1142 and the other subsynchronous binaries will be extremely useful for constraining mass and angular momentum transfer.

ACKNOWLEDGEMENTS

Funding for this research was provided by the National Science Foundation grant#1312869. Any opinions, findings, and conclusions or recommendations expressed in this material are those of the author(s) and do not necessarily reflect the views of the National Science Foundation. JK, LR, AW, and HF were supported by the Missouri Space Grant Consortium, funded by NASA. ASB gratefully acknowledges a financial support from the Polish National Science Center under project No. UMO-2011/03/D/ST9/01914. This paper includes data collected by the *Kepler* mission. Funding for the *Kepler* mission is provided by the NASA Science Mission directorate. Data presented in this paper were obtained from the Mikulski Archive for Space Telescopes (MAST). STScI is operated by the Association of Universities for Research in Astronomy, Inc., under NASA contract NAS5-26555. Support for MAST for non-HST data is provided by the NASA Office of Space Science via grant NNX13AC07G and by other grants and contracts.

The spectroscopic observations used in this work were obtained with the Nordic Optical Telescope at the Observatorio del Roque de los Muchachos and operated jointly by Denmark, Finland, Iceland, Norway, and Sweden and the Mayall Telescope of KPNO, which is operated by the Association of Universities for Research in Astronomy under cooperative agreement with the National Science Foundation.

REFERENCES

Aerts C., Christensen-Dalsgaard J., Kurtz D. W., 2010, Asteroseismology. Springer-Verlag, Berlin
Baran A. S., Winans A., 2012, Acta Astron., 62, 343
Baran A. S. et al., 2012, MNRAS, 424, 2686
Baran A. S., Koen C., Pokrzywka B., 2015, MNRAS, 448, L16
Bevington P. R., Robinson D. K., 2003, Data reduction and Error Analysis for the Physical Sciences. McGraw-Hill, New York
Bloemen S. et al., 2011, MNRAS, 410, 1787
Copperwheat C. M., Marsh T. R., Dhillon V. S., Littlefair S. P., Hickman R., Gänsicke B. T., Southworth J., 2010, MNRAS, 402, 1824
Foster H. M., Reed M. D., Telting J. H., Østensen R. H., Baran A. S., 2015, ApJ, 805, 94
Green R. F., Schmidt M., Liebert J., 1986, ApJS, 61, 305
Heber U., Reid I. N., Werner K., 1999, A&A, 348, L25
Howell S. B. et al., 2014, PASP, 126, 398
Jeffery C. S., Ramsay G., 2014, MNRAS, 442, L61
Martin D. C. et al., 2005, ApJ, 619, L1
Pablo H., Kawaler S. D., Green E. M., 2011, ApJ, 740, L47
Pablo H. et al., 2012, MNRAS, 422, 1343
Reed M., Foster H., 2014, in van Grootel V., Green E., Fontaine G., Charpinet S., eds, ASP Conf. Ser. Vol. 481, 6th Meeting on Hot Subdwarf Stars and Related Objects. Astron. Soc. Pac., San Francisco, p. 45
Reed M. D., Stiening R., 2004, PASP, 116, 506
Reed M. D. et al., 2004, MNRAS, 348, 1164
Reed M. D. et al., 2007, ApJ, 664, 518
Reed M. D. et al., 2011, MNRAS, 414, 2885
Reed M. D., Foster H., Telting J. H., Østensen R. H., Farris L. H., Oreiro R., Baran A. S., 2014, MNRAS, 440, 3809
Still M., Barclay T., 2012, Astrophysics Source Code Library, record ascl:1208.004
Telting J. H. et al., 2012, A&A, 544, A1
Telting J., Østensen R., Reed M., Kiæerad F., Farris L., Baran A., Oreiro R., O'Toole S., 2014a, in van Grootel V., Green E., Fontaine G., Charpinet S., eds, ASP Conf. Ser. Vol. 481, 6th Meeting on Hot Subdwarf Stars and Related Objects. Astron. Soc. Pac., San Francisco, p. 287
Telting J. H. et al., 2014b, A&A, 570, A129
Østensen R. H. et al., 2010, MNRAS, 409, 1470
Østensen R. H. et al., 2011, MNRAS, 414, 2860
Østensen R. H., Reed M. D., Baran A. S., Telting J. H., 2014a, A&A, 564, L14
Østensen R. H., Telting J. H., Reed M. D., Baran A. S., Nemeth P., Kiaeerad F., 2014b, A&A, 569, A15

This paper has been typeset from a TEX/LATEX file prepared by the author.